

Terahertz Spectroscopy of Dilute Gases Using $\text{Bi}_2\text{Sr}_2\text{CaCu}_2\text{O}_{8+\delta}$ Intrinsic Josephson-Junction Stacks

Hancong Sun,^{1,2} Zhibao Yang,¹ Nickolay V. Kinev,³ Oleg S. Kiselev,³ Yangyang Lv,¹ Ya Huang,^{1,2} Luyao Hao,^{1,2} Xianjing Zhou,^{1,2} Min Ji,^{1,2} Xuecou Tu,¹ Caihong Zhang,¹ Jun Li,¹ Fabian Rudau,⁴ Raphael Wieland,⁴ Johannes S. Hampp,⁴ Olcay Kizilaslan,^{4,5} Dieter Koelle,⁴ Biaobing Jin,¹ Jian Chen,¹ Lin Kang,¹ Weiwei Xu,¹ Reinhold Kleiner,^{4,†} Valery P. Koshelets,³ Huabing Wang,^{1,*} and Peiheng Wu¹

¹Research Institute of Superconductor Electronics, Nanjing University, Nanjing 210023, China

²National Institute for Materials Science, Tsukuba 305-0047, Japan

³Kotelnikov Institute of Radio Engineering and Electronics, Moscow 125009, Russia

⁴Physikalisches Institut and Center for Quantum Science in LISA⁺, Universität Tübingen, D-72076 Tübingen, Germany

⁵Department of Biomedical Engineering, Faculty of Engineering, Inonu University, 44280 Malatya, Turkey

(Received 30 July 2017; published 3 November 2017)

We report on spectrometric gas detection using terahertz waves radiated from $\text{Bi}_2\text{Sr}_2\text{CaCu}_2\text{O}_{8+\delta}$ (BSCCO) intrinsic Josephson-junction stacks. The emission frequency is varied by changing the bias current through and thus the voltage across the emitter. For the terahertz detection, both bolometric and heterodyne detection methods are employed. Clear absorption dips of water and ammonia vapor on the terahertz spectrum are obtained with both detection methods. With the bolometric scheme, we achieve a frequency resolution of about 1 GHz, which is on the order of the frequency resolution of systems employing terahertz time-domain spectroscopy. With the more stable heterodyne detection scheme, the minimum detectable gas pressure is around 0.001 mbar for H_2O and about 0.07 mbar for NH_3 . The smallest observable absorption linewidths are in the range of 4 to 5 MHz. Our results suggest that the frequency-tunable BSCCO emitters can be convenient sources for potential terahertz applications in spectroscopy for frequencies between roughly 0.4 and 2 THz.

DOI: 10.1103/PhysRevApplied.8.054005

I. INTRODUCTION

Terahertz science and technology has been a hot topic for decades due to potential applications in detection and imaging, such as environmental monitoring, high-bandwidth communication technologies, medical diagnostics, public security, and food quality control [1,2]. A variety of sources of terahertz radiation have been reported [1]. For example, in terms of compact solid-state devices, there are powerful quantum cascade lasers for frequencies above 1.5 THz [3,4]. For frequencies between 0.5 and 1.5 THz, resonant-tunneling diodes look promising, reaching power levels in the microwatt range [5,6]. In this paper, we focus on terahertz emitters based on the high-critical-temperature (T_c) superconductor $\text{Bi}_2\text{Sr}_2\text{CaCu}_2\text{O}_{8+\delta}$ (BSCCO) operating at frequencies of between 0.4 and 2.4 THz [7–9]. These oscillators are based on the ac Josephson effect.

A unit cell of BSCCO consists of superconducting CuO_2 layers and insulating BiO and SrO layers, resulting in natural (intrinsic) Josephson junctions along the c axis [10]. A single crystal of 1.5 μm thickness forms a stack of

$N \sim 1000$ of such intrinsic Josephson junctions (IJJs). If the voltage across all IJJs is the same, the junctions oscillate at a frequency $f_J = 2eV/hN$, where e is the elementary charge, h is the Planck constant, and V is the voltage across the whole stack. Coherent off-chip terahertz emission is first demonstrated for 1- μm -thick BSCCO stacks, with an extrapolated output power of up to 0.5 μW for frequencies of between 0.5 and 0.85 THz [11]. Phase synchronization of the IJJs is reached through cavity resonances excited in the stack. Terahertz emission from BSCCO stacks is under intensive experimental [11–41] and theoretical [42–65] research and has led to several demonstrations of applications, such as terahertz absorption and reflection imaging [25,33,40] or an all-high- T_c integrated receiver [26]. IJJ stacks have been patterned as mesas on top of BSCCO base crystals, as bare IJJ stacks contacted by Au layers [gold-BSCCO-gold (GBG) structures] [24,26,29,31] and as all-superconducting Z-shaped structures [21]. For the best stacks, an emission power P_e in the range of tens of microwatts has been achieved [26,28,29,35], and arrays of mesas showed emission with P_e values of up to 0.61 mW [28]. Emission frequencies range from 0.4 to 2.4 THz [9,31,34,35]; however, above about 2 THz, the emission power decreases strongly.

*hbwang@nju.edu.cn

†kleiner@uni-tuebingen.de

The IJJ stacks are affected by Joule heating. For sufficiently low bias currents, the temperature rises only slightly to values above the bath temperature T_b , and the voltage V across the stack increases with an increasing bias current I . With increasing I values and input power, the current-voltage characteristics (IVC) starts to backbend and, at a certain bias current in the backbending region, a hot spot forms in the stack, creating a region which is heated to temperatures above T_c . In the IJJ stacks, one can thus distinguish a low-bias regime where the temperature in the stack varies only weakly and a high-bias regime where the hot spot has formed. Terahertz emission can be observed in both regimes. While the reported linewidth of radiation is not smaller than 0.5 GHz at low bias [22,24], in the high-bias regime it can be as narrow as 7 MHz [22,66].

It is of interest to study to what extent IJJ stacks can be used for spectroscopy purposes. Thus, in this work, sweeping the emission frequency of BSCCO emitters by varying the bias current, we measure terahertz absorption spectra of water and ammonia vapor. In a first, proof-of-principle experiment, we detect the terahertz radiation bolometrically. In a second and more elaborate experiment, we monitor the terahertz absorption characteristics of the two gases by a heterodyne-mixing detection method. Here, a 5-MHz (4-MHz) linewidth of the absorption signal of ammonia vapor is observed at a pressure p of 0.23 mbar (0.07 mbar).

II. MEASUREMENTS

The emitter is fabricated as a GBG structure from a BSCCO single crystal which is annealed at 650 °C, 18 Pa Ar, and 2 Pa O₂ for 48 h. After annealing, the critical temperature T_c is approximately 89 K. The microfabrication process is described in Ref. [26]. The resulting rectangular IJJ stack has an in-plane size of $(300 \times 50) \mu\text{m}^2$ and a thickness of 1.1 μm , corresponding to approximately 730 IJJs in series. The emitter is shown schematically in Fig. 1(a). For electrical contact, two gold wires are connected to the electrodes by silver epoxy.

In a first and very simple experiment, we use the gas-detection system shown in Fig. 1. Using GE varnish, the MgO substrate hosting the BSCCO emitter is glued onto a hemispherical sapphire lens. No special measures are taken into account for thermal management or impedance mismatch between the sample, the substrate, and the lens. Then the emitter is placed in a Stirling cryocooler (RICOR K535) which can cool down to 30 K from room temperature. The temperature is detected by a DT-670 silicon diode. The emission is directed to a 52-cm-long gas cell via an off-axis parabolic mirror, where both windows of the cell are made of 2-mm-thick terahertz-transparent Teflon. The terahertz beam is modulated by a mechanical chopper (with a modulation frequency of 14 Hz) and detected with a TYDEX GC-1P Golay cell. This cell is read out by a lock-in amplifier and calibrated against the response of a Si bolometer that is calibrated using a blackbody radiation source. The gas

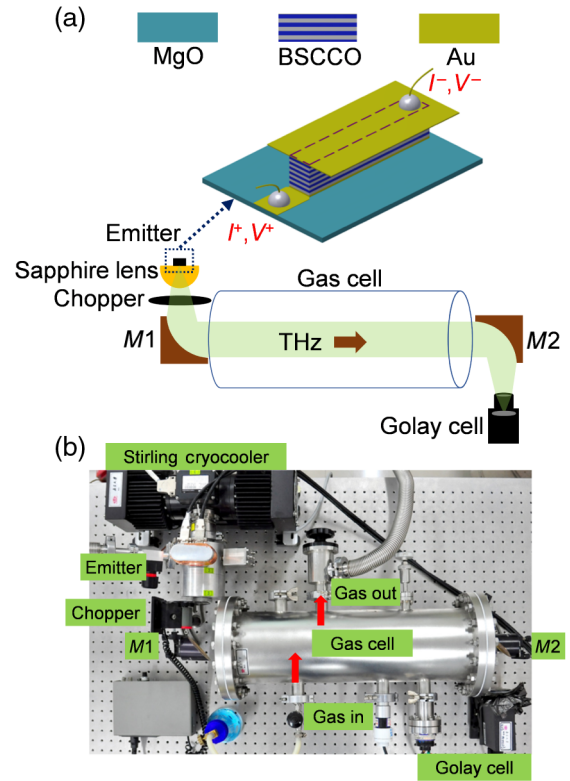


FIG. 1. (a) Sketch and (b) photograph of the terahertz gas-detection system with BSCCO intrinsic Josephson junctions as a tunable terahertz emitter. $M1$ and $M2$ denote parabolic mirrors. The IJJ stack forming a GBG structure is shown at the top of the sketch.

chamber is initially pumped out to a pressure of 3×10^{-5} mbar, and the target gas is then directed into the chamber via a gas valve. Here, we should note that the ammonia vapor used for the experiment volatilizes from ammonia water and contains additional water vapor with a proportion of less than 10%. The terahertz beam goes partially through air, also causing absorption due to water. The environmental humidity is about 40%. To change the emission frequency of the terahertz source, we simply vary the bias current through the IJJ stack, leading to a change in voltage V and, consequently, in f_J . To determine the frequency of the emitted radiation, a homemade Fourier spectrometer [67] is inserted into the beam path. For further evaluation, V is monitored and converted to frequency using this calibration and the proportionality of f_J and V . In a second experiment, we operate the emitter in a helium-cooled optical cryostat and use a helium-cooled superconducting integrated receiver instead of the Golay cell to directly detect the emission power and frequency by heterodyne mixing. The setup is similar to the one shown in Ref. [68].

III. RESULTS

Figure 2 shows the IVC of the stack, as measured at a bath temperature $T_b = 30$ K. The contact resistance

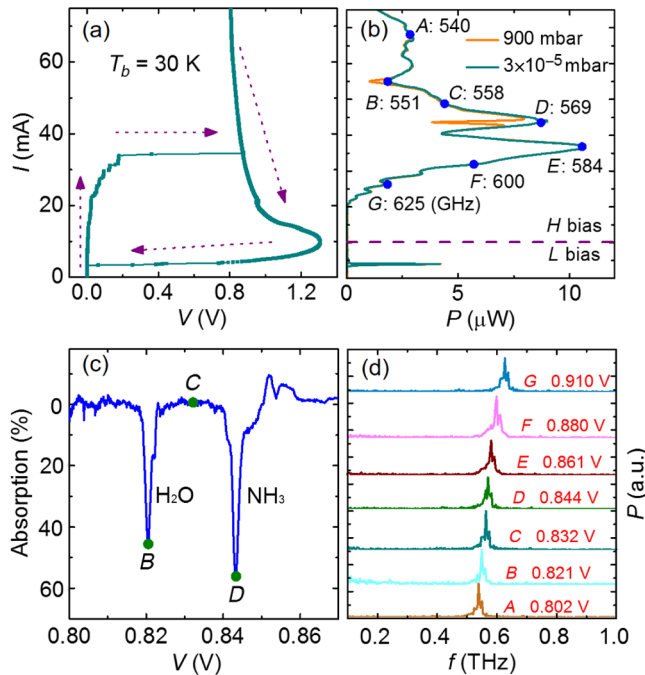


FIG. 2. (a) IVC of the emitter, as measured at a bath temperature $T_b = 30$ K. Dashed lines indicate the current sweep sequence. (b) Emission power detected by the Golay cell as a function of I for the evacuated gas cell ($p = 3 \times 10^{-5}$ mbar) and for the cell filled with ammonia vapor at a pressure of 900 mbar. (c) Absorption, as calculated from a ratio of the spectra at $p = 900$ mbar and $p = 3 \times 10^{-5}$ mbar, as a function of voltage V across the stack. (d) Fourier spectra of the emitted radiation for the bias points (A) to (G) indicated in (b). The widths of the emission peaks seen here are resolution limited by the maximum displacement of the two split mirrors used in the spectrometer. The peak positions vary from 540 to 625 GHz, which covers the range of the rotational frequencies of interest of ammonia and water molecules. From these data, we also find a number N of 710 ± 10 IJJs contributing to the emission peaks, which roughly corresponds to the number of IJJs estimated from the thickness of the stack.

between the IJJ stack and the contacting gold layers is subtracted. Dashed lines in the graph indicate the current sweep sequence. All junctions switch to their resistive states when the bias current exceeds 34.5 mA. By further increasing I to 75 mA and then back to zero, the IVC in the fully resistive state is obtained, exhibiting the typical heating-induced S shape. The highest voltage across the stack is 1.31 V. Figure 2(b) shows—as a function of I , by the dark-cyan line—the emission power, as detected by the Golay cell, for the case of an evacuated gas cell ($p = 3 \times 10^{-5}$ mbar).

In the high-bias regime, where the differential resistance of the IVC is negative, the stack emits in the current range 20–75 mA, covering a voltage range of 0.805 to 0.956 V. The highest detected emission power occurs at $I = 36.76$ mA [point E in Fig. 2(b)] and amounts to about 10.6μ W. The emission observed is stable over time but exhibits several peaks as a function of I , presumably because different resonant modes are excited at different currents [11,12,17,18,24]. There is also an emission peak at low bias, at a current near 5 mA. We do not evaluate this

peak further since our focus is on the high-bias regime, providing a much broader and more stable regime to tune our device by current. The orange line in Fig. 2(b) displays the detected terahertz emission for an ammonia pressure of 900 mbar. While, over large current ranges, this curve coincides with the background curve measured at 3×10^{-5} mbar gas pressure, at currents near 40 and 55 mA, the two curves deviate. To show this difference more clearly, we plot in Fig. 2(c) the absorption, calculated from the ratio of the two curves of Fig. 2(b), as a function of V . Two absorption dips are clearly visible, where, in fact, one is from the water vapor and the other from ammonia.

Note that there is also an “emission” peak between 0.85 and 0.86 V. This is actually an artifact arising from the steep gradients in the terahertz emission spectra visible in Fig. 2(b) between bias points D and E. In principle, the voltage V across the stack could be directly converted to frequency if the number of IJJs participating in radiation and the contact resistance were known exactly. As this is not the case, we measure, for the evacuated gas cell, emission spectra using our homemade Fourier spectrometer. Some spectra, as detected for the bias points A–G in Fig. 2(b), are shown in Fig. 2(d). The widths of the emission peaks seen here are resolution limited by the maximum displacement of the two split mirrors used in the spectrometer. The peak positions vary from 540 to 625 GHz, which covers the range of the rotational frequencies of interest of ammonia and water molecules. From these data, we also find a number N of 710 ± 10 IJJs contributing to the emission peaks, which roughly corresponds to the number of IJJs estimated from the thickness of the stack.

Figure 3 shows the terahertz absorption spectra of ammonia and water vapor at different gas pressures, calculated from the ratio of the various P -vs- V curves to the P -vs- V background curve obtained for the evacuated gas cell. At the highest pressures, the widths of the absorption lines of the two gases are very large (about 2 mV), which is expected due to collisional broadening. However, for lower pressures, the linewidths decrease mildly, reaching values of around 1.2–1.4 mV for pressures below 20 mbar and showing that the resolution (in voltage) of the absorption lines is limited by noise in the setup. For ammonia vapor, as shown in Fig. 3(a), the absorption center of the curves is at $V = 0.843$ V, where the frequency, measured with our interferometer, is about 569 GHz. This is close to the well-known rotational-transition frequency ($f = 572.5$ GHz) of ammonia molecules. We use this value and the Josephson relation to recalibrate the frequency axis in Fig. 3(a) and to obtain a more precise value for the number of emitting IJJs, $N = 712$.

For water-vapor absorption, as shown in Fig. 3(b), the same calculation also yields $N = 712$, confirming that we can perform gas spectroscopy—at least in principle—by sweeping the current and monitoring the voltage of the

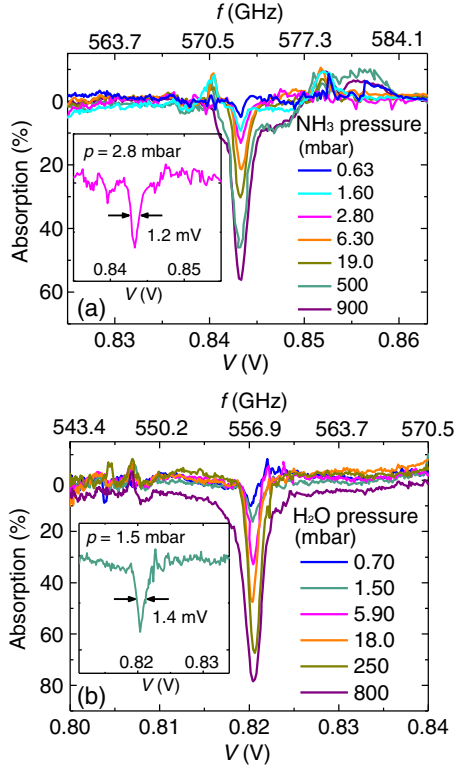


FIG. 3. Terahertz absorption signal vs voltage across the stack for different pressures of (a) ammonia vapor and (b) water vapor. The frequency displayed at the upper abscissa is calculated via the Josephson relation $f = 2eV/hN$, with $N = 712$. The inset in (a) shows the NH_3 absorption spectrum at $p = 2.8$ mbar, and the inset in (b) the H_2O absorption spectrum at $p = 1.5$ mbar.

BSCCO emitter. The minimum pressure of the ammonia vapor where we can still observe the absorption dip is 0.63 mbar. The inset in Fig. 3(a) shows the absorption signal vs V at $p = 2.8$ mbar, with a maximum absorption of about 13.1%. Here, the measured linewidth of the absorption curves is 1.2 mV, corresponding to about 0.82 GHz. For water [see the inset in Fig. 3(b)], we can safely detect the absorption line down to $p = 0.7$ mbar, and the minimal linewidth is about 1.4 mV (0.95 GHz), which is already comparable to the frequency resolution of systems used in time-domain spectroscopy [69].

For further improvement, in our second experiment, to accurately measure the terahertz absorption spectra of ammonia and water vapor, a Nb-AlN-NbN superconducting integrated receiver (SIR) [66], with an effective frequency detection range of 450 to 700 GHz and a confirmed frequency resolution well below 100 kHz is employed as a detector [66,70]. The SIR was used previously to study terahertz emission from IJJ stacks [22] and to perform gas detection [66,68,71,72]. In the present experiment, the bias current through the BSCCO emitter is kept at a constant value, tuned to the respective gas-line frequency, and intermediate-frequency spectra are taken using the SIR. Measurements are done at $T_b = 4.2$ K, where the linewidth

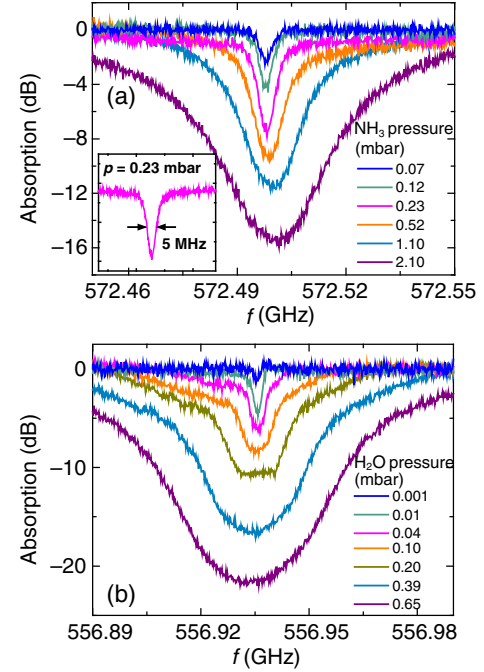


FIG. 4. (a) Terahertz absorption spectra of ammonia (mixed with water; 10% solution) and (b) water vapor at different pressures by a BSCCO emitter and a SIR terahertz detector. The emitter and the SIR are operated at $T_b = 4.2$ K. The empty-cell curve is subtracted from the data. (Inset) An absorption spectrum of ammonia vapor at $p = 0.23$ mbar, with an absorption linewidth of 5 MHz.

of radiation of the emitter is 60 MHz at 572.5 GHz (NH_3) and 57 MHz at 557 GHz (H_2O). With this setup, high-resolution terahertz absorption spectra of ammonia and water vapor are, as in Ref. [68], achieved in a narrow frequency band lower than the linewidth of the BSCCO emitter; see Fig. 4 [73]. The emitter, operated in a free-running mode, is stable enough to permit this kind of measurement. As in Fig. 3, the absorption lines of ammonia and water are highly broadened at large gas pressures, with the linewidth decreasing with decreasing pressure. For ammonia, at $p = 0.23$ mbar, which is the order of the concentration of trace gases, a clear absorption dip with an absorption linewidth of about 5 MHz is observed, as shown in the inset of Fig. 4(a). At $p = 0.07$ mbar, the measured linewidth is 4 MHz (although affected by Doppler broadening, which we do not further analyze here).

The observed rotation frequencies of ammonia (572.498 GHz) and water (556.936 GHz) coincide with literature values. Further improvement of the lowest resolvable linewidth is possible by using proper feedback techniques for the oscillator [70].

IV. CONCLUSIONS

In this work, using terahertz waves generated from BSCCO IJJ stacks, we record terahertz absorption spectra

of ammonia vapor near 572 GHz and water vapor near 557 GHz using two different setups. The first experiment uses a very simple terahertz transmission gas-detection system based on the bolometric detection of the terahertz emission signal. The emitter is cooled by a Stirling cryocooler. Clear absorption dips at different gas pressures are observed by simply sweeping the bias current and monitoring the voltage across the stacks; however, the setup is not stable enough to resolve the absorption linewidths at low pressures.

In the second experiment, we measure terahertz absorption characteristics of the two gases using a superconducting integrated receiver for detecting the terahertz power and frequency. The emitter and the receiver are mounted in different helium-cooled cryostats. With this setup, we achieve minimum absorption linewidths of 4 to 5 MHz at pressures well below 0.1 mbar. Of course, the performance is still far below the sensitivity and frequency resolution of the most sophisticated detection schemes based on chirped-pulse Fourier-transform spectroscopy [74]. However, it is not so different from quantum-cascade-laser-based schemes realized for gas sensing in the 2- to 3-THz range [75]. BSCCO emitters are suitable candidates for terahertz spectroscopy for frequencies of between about 0.4 and 2 THz and can be used for applications in environmental monitoring.

ACKNOWLEDGMENTS

We gratefully acknowledge financial support from the National Natural Science Foundation of China (Grants No. 11234006, No. 61611130069, No. 11227904, No. 61371036, No. 61521001, and No. 61501220), the Fundamental Research Funds for the Central Universities and Jiangsu Key Laboratory of Advanced Techniques for Manipulating Electromagnetic Waves, the Priority Academic Program Development of Jiangsu Higher Education Institutions (PAPD), the Jiangsu Provincial Natural Science Fund (Grant No. BK20150561), RFBR Grant No. 17-52-12051, and the Deutsche Forschungsgemeinschaft via Project No. KL930-13/2.

[1] M. Tonouchi, Cutting-edge terahertz technology, *Nat. Photonics* **1**, 97 (2007).
 [2] B. Ferguson and X.C. Zhang, Materials for terahertz science and technology, *Nat. Mater.* **1**, 26 (2002).
 [3] B.S. Williams, Terahertz quantum-cascade lasers, *Nat. Photonics* **1**, 517 (2007).
 [4] S. Kumar, Recent progress in terahertz quantum cascade lasers, *IEEE J. Sel. Top. Quantum Electron.* **17**, 38 (2011).
 [5] M. Feiginov, H. Kanaya, S. Suzuki, and M. Asada, Operation of resonant-tunneling diodes with strong back injection from the collector at frequencies up to 1.46 THz, *Appl. Phys. Lett.* **104**, 243509 (2014).

[6] S. Suzuki, M. Asada, A. Teranishi, H. Sugiyama, and H. Yokoyama, Fundamental oscillation of resonant tunneling diodes above 1 THz at room temperature, *Appl. Phys. Lett.* **97**, 242102 (2010).
 [7] U. Welp, K. Kadowaki, and R. Kleiner, Superconducting emitters of THz radiation, *Nat. Photonics* **7**, 702 (2013).
 [8] I. Kakeya and H. B. Wang, Terahertz-wave emission from Bi2212 intrinsic Josephson junctions: A review on recent progress, *Supercond. Sci. Technol.* **29**, 073001 (2016).
 [9] T. Kashiwagi, H. Kubo, K. Sakamoto, T. Yuasa, Y. Tanabe, C. Watanabe, T. Tanaka, Y. Komori, R. Ota, G. Kuwano, K. Nakamura, T. Katsuragawa, M. Tsujimoto, T. Yamamoto, R. Yoshizaki, H. Minami, K. Kadowaki, and R. A. Klemm, The present status of high- T_c superconducting terahertz emitters, *Supercond. Sci. Technol.* **30**, 074008 (2017).
 [10] R. Kleiner, F. Steinmeyer, G. Kunkel, and P. Müller, Intrinsic Josephson Effects in Bi₂Sr₂CaCu₂O₈ Single Crystals, *Phys. Rev. Lett.* **68**, 2394 (1992).
 [11] L. Ozyuzer, A. E. Koshelev, C. Kurter, N. Gopalsami, Q. Li, M. Tachiki, K. Kadowaki, T. Yamamoto, H. Minami, H. Yamaguchi, T. Tachiki, K. E. Gray, W.-K. Kwok, and U. Welp, Emission of coherent THz radiation from superconductors, *Science* **318**, 1291 (2007).
 [12] H. B. Wang, S. Guénon, J. Yuan, A. Iishi, S. Arisawa, T. Hatano, T. Yamashita, D. Koelle, and R. Kleiner, Hot Spots and Waves in Bi₂Sr₂CaCu₂O₈ Intrinsic Josephson Junction Stacks: A Study by Low Temperature Scanning Laser Microscopy, *Phys. Rev. Lett.* **102**, 017006 (2009).
 [13] H. Minami, I. Kakeya, H. Yamaguchi, T. Yamamoto, and K. Kadowaki, Characteristics of terahertz radiation emitted from the intrinsic Josephson junctions in high- T_c superconductor Bi₂Sr₂CaCu₂O_{8+δ}, *Appl. Phys. Lett.* **95**, 232511 (2009).
 [14] K. E. Gray, L. Ozyuzer, A. E. Koshelev, C. Kurter, K. Kadowaki, T. Yamamoto, H. Minami, H. Yamaguchi, M. Tachiki, W.-K. Kwok, and U. Welp, Emission of terahertz waves from stacks of intrinsic Josephson junctions, *IEEE Trans. Appl. Supercond.* **19**, 886 (2009).
 [15] S. Guénon, M. Grünzweig, B. Gross, J. Yuan, Z. G. Jiang, Y. Y. Zhong, M. Y. Li, A. Iishi, P. H. Wu, T. Hatano, R. G. Mints, E. Goldobin, D. Koelle, H. B. Wang, and R. Kleiner, Interaction of hot spots and THz waves in Bi₂Sr₂CaCu₂O₈ intrinsic Josephson junction stacks of various geometry, *Phys. Rev. B* **82**, 214506 (2010).
 [16] C. Kurter, L. Ozyuzer, T. Proslir, J. F. Zasadzinski, D. G. Hinks, and K. E. Gray, Counterintuitive consequence of heating in strongly-driven intrinsic junctions of Bi₂Sr₂CaCu₂O_{8+δ} mesas, *Phys. Rev. B* **81**, 224518 (2010).
 [17] H. B. Wang, S. Guénon, B. Gross, J. Yuan, Z. G. Jiang, Y. Y. Zhong, M. Grünzweig, A. Iishi, P. H. Wu, T. Hatano, D. Koelle, and R. Kleiner, Coherent Terahertz Emission of Intrinsic Josephson Junction Stacks in the Hot Spot Regime, *Phys. Rev. Lett.* **105**, 057002 (2010).
 [18] M. Tsujimoto, K. Yamaki, K. Deguchi, T. Yamamoto, T. Kashiwagi, H. Minami, M. Tachiki, K. Kadowaki, and R. A. Klemm, Geometrical Resonance Conditions for THz Radiation from the Intrinsic Josephson Junctions in Bi₂Sr₂CaCu₂O_{8+δ}, *Phys. Rev. Lett.* **105**, 037005 (2010).
 [19] H. Koseoglu, F. Turkoglu, Y. Simsek, and L. Ozyuzer, The fabrication of THz emitting mesas by reactive ion-beam

- etching of superconducting Bi2212 with multilayer masks, *J. Supercond. Novel Magn.* **24**, 1083 (2011).
- [20] T. M. Benseman, A. E. Koshelev, K. E. Gray, W.-K. Kwok, U. Welp, K. Kadowaki, M. Tachiki, and T. Yamamoto, Tunable terahertz emission from $\text{Bi}_2\text{Sr}_2\text{CaCu}_2\text{O}_{8+\delta}$ mesa devices, *Phys. Rev. B* **84**, 064523 (2011).
- [21] J. Yuan, M. Y. Li, J. Li, B. Gross, A. Ishii, K. Yamaura, T. Hatano, K. Hirata, E. Takayama Muromachi, P. H. Wu, D. Koelle, R. Kleiner, and H. B. Wang, Terahertz emission from $\text{Bi}_2\text{Sr}_2\text{CaCu}_2\text{O}_{8+\delta}$ intrinsic Josephson junction stacks with all-superconducting electrodes, *Supercond. Sci. Technol.* **25**, 075015 (2012).
- [22] M. Y. Li, J. Yuan, N. Kinev, J. Li, B. Gross, S. Guénon, A. Ishii, K. Hirata, T. Hatano, D. Koelle, R. Kleiner, V. P. Koshelets, H. B. Wang, and P. H. Wu, Linewidth dependence of coherent terahertz emission from $\text{Bi}_2\text{Sr}_2\text{CaCu}_2\text{O}_8$ intrinsic Josephson junction stacks in the hot-spot regime, *Phys. Rev. B* **86**, 060505(R) (2012).
- [23] I. Kakeya, Y. Omukai, T. Yamamoto, K. Kadowaki, and M. Suzuki, Effect of thermal inhomogeneity for terahertz radiation from intrinsic Josephson junction stacks of $\text{Bi}_2\text{Sr}_2\text{CaCu}_2\text{O}_{8+\delta}$, *Appl. Phys. Lett.* **100**, 242603 (2012).
- [24] T. Kashiwagi, M. Tsujimoto, T. Yamamoto, H. Minami, K. Yamaki, K. Delfanzari, K. Deguchi, N. Orita, T. Koike, R. Nakayama, T. Kitamura, M. Sawamura, S. Hagino, K. Ishida, K. Ivancovic, H. Asai, M. Tachiki, R. A. Klemm, and K. Kadowaki, High temperature superconductor terahertz emitters: Fundamental physics and its applications, *J. Appl. Phys.* **51**, 010113 (2012).
- [25] M. Tsujimoto, H. Minami, K. Delfanzari, M. Sawamura, R. Nakayama, T. Kitamura, T. Yamamoto, T. Kashiwagi, T. Hattori, and K. Kadowaki, Terahertz imaging system using high- T_c superconducting oscillation devices, *J. Appl. Phys.* **111**, 123111 (2012).
- [26] D. Y. An *et al.*, Terahertz emission and detection both based on high- T_c superconductors: Towards an integrated receiver, *Appl. Phys. Lett.* **102**, 092601 (2013).
- [27] T. M. Benseman, A. E. Koshelev, W.-K. Kwok, U. Welp, V. K. Vlasko-Vlasov, K. Kadowaki, H. Minami, and C. Watanabe, Direct imaging of hot spots in $\text{Bi}_2\text{Sr}_2\text{CaCu}_2\text{O}_{8+\delta}$ mesa terahertz sources, *J. Appl. Phys.* **113**, 133902 (2013).
- [28] T. M. Benseman, K. E. Gray, A. E. Koshelev, W.-K. Kwok, U. Welp, H. Minami, K. Kadowaki, and T. Yamamoto, Powerful terahertz emission from $\text{Bi}_2\text{Sr}_2\text{CaCu}_2\text{O}_{8+\delta}$ mesa arrays, *Appl. Phys. Lett.* **103**, 022602 (2013).
- [29] S. Sekimoto, C. Watanabe, H. Minami, T. Yamamoto, T. Kashiwagi, R. A. Klemm, and K. Kadowaki, Continuous 30 μW terahertz source by a high- T_c superconductor mesa structure, *Appl. Phys. Lett.* **103**, 182601 (2013).
- [30] H. Minami, C. Watanabe, K. Sato, S. Sekimoto, T. Yamamoto, T. Kashiwagi, R. A. Klemm, and K. Kadowaki, Local SiC photoluminescence evidence of hot spot formation and sub-THz coherent emission from a rectangular $\text{Bi}_2\text{Sr}_2\text{CaCu}_2\text{O}_{8+x}$ mesa, *Phys. Rev. B* **89**, 054503 (2014).
- [31] M. Ji *et al.*, $\text{Bi}_2\text{Sr}_2\text{CaCu}_2\text{O}_8$ intrinsic Josephson junction stacks with improved cooling: Coherent emission above 1 THz, *Appl. Phys. Lett.* **105**, 122602 (2014).
- [32] T. Kashiwagi, K. Nakade, Y. Saiwai, H. Minami, T. Kitamura, C. Watanabe, K. Ishida, S. Sekimoto, K. Asanuma, T. Yasui, Y. Shibano, M. Tsujimoto, T. Yamamoto, B. Markovic, J. Mirkovic, R. A. Klemm, and K. Kadowaki, Computed tomography image using sub-terahertz waves generated from a high- T_c superconducting intrinsic Josephson junction oscillator, *Appl. Phys. Lett.* **104**, 082603 (2014).
- [33] T. Kashiwagi, K. Nakade, B. Markovic, Y. Saiwai, H. Minami, T. Kitamura, C. Watanabe, K. Ishida, S. Sekimoto, K. Asanuma, T. Yasui, Y. Shibano, M. Tsujimoto, T. Yamamoto, J. Mirkovic, and K. Kadowaki, Reflection type of terahertz imaging system using a high- T_c superconducting oscillator, *Appl. Phys. Lett.* **104**, 022601 (2014).
- [34] T. Kashiwagi, T. Yamamoto, T. Kitamura, K. Asanuma, C. Watanabe, K. Nakade, T. Yasui, Y. Saiwai, Y. Shibano, H. Kubo, K. Sakamoto, T. Katsuragawa, M. Tsujimoto, K. Delfanzari, R. Yoshizaki, H. Minami, R. A. Klemm, and K. Kadowaki, Generation of electromagnetic waves from 0.3 to 1.6 terahertz with a high- T_c superconducting $\text{Bi}_2\text{Sr}_2\text{CaCu}_2\text{O}_{8+\delta}$ intrinsic Josephson junction emitter, *Appl. Phys. Lett.* **106**, 092601 (2015).
- [35] T. Kashiwagi, K. Sakamoto, H. Kubo, Y. Shibano, T. Enomoto, T. Kitamura, K. Asanuma, T. Yasui, C. Watanabe, K. Nakade, Y. Saiwai, T. Katsuragawa, M. Tsujimoto, R. Yoshizaki, T. Yamamoto, H. Minami, R. A. Klemm, and K. Kadowaki, A high- T_c intrinsic Josephson junction emitter tunable from 0.5 to 2.4 terahertz, *Appl. Phys. Lett.* **107**, 082601 (2015).
- [36] X. J. Zhou, Q. Zhu, M. Ji, D. Y. An, L. Y. Hao, H. C. Sun, S. Ishida, F. Rudau, R. Wieland, J. Li, D. Koelle, H. Eisaki, Y. Yoshida, T. Hatano, R. Kleiner, H. B. Wang, and P. H. Wu, Three-terminal stand-alone superconducting terahertz emitter, *Appl. Phys. Lett.* **107**, 122602 (2015).
- [37] L. Y. Hao, M. Ji, J. Yuan, D. Y. An, M. Y. Li, X. J. Zhou, Y. Huang, H. C. Sun, Q. Zhu, F. Rudau, R. Wieland, N. Kinev, J. Li, W. W. Xu, B. B. Jin, J. Chen, T. Hatano, V. P. Koshelets, D. Koelle, R. Kleiner, H. B. Wang, and P. H. Wu, Compact Superconducting Terahertz Source Operating in Liquid Nitrogen, *Phys. Rev. Applied* **3**, 024006 (2015).
- [38] T. Kashiwagi *et al.*, Efficient Fabrication of Intrinsic-Josephson-Junction Terahertz Oscillators with Greatly Reduced Self-Heating Effects, *Phys. Rev. Applied* **4**, 054018 (2015).
- [39] C. Watanabe, H. Minami, T. Kitamura, K. Asanuma, K. Nakade, T. Yasui, Y. Saiwai, Y. Shibano, T. Yamamoto, T. Kashiwagi, R. A. Klemm, and K. Kadowaki, Influence of the local heating position on the terahertz emission power from high- T_c superconducting $\text{Bi}_2\text{Sr}_2\text{CaCu}_2\text{O}_{8+\delta}$ mesas, *Appl. Phys. Lett.* **106**, 042603 (2015).
- [40] K. Nakade, T. Kashiwagi, Y. Saiwai, H. Minami, T. Yamamoto, R. A. Klemm, and K. Kadowaki, Applications using high- T_c superconducting terahertz emitters, *Sci. Rep.* **6**, 23178 (2016).
- [41] M. Tsujimoto, Y. Maeda, A. Elarabi, Y. Yoshioka, Y. Nakagawa, Y. Wen, T. Doi, H. Saito, and I. Kakeya, Cavity mode identification for coherent terahertz emission from high- T_c superconductors, *Opt. Express* **24**, 4591 (2016).
- [42] L. N. Bulaevskii and A. E. Koshelev, Radiation due to Josephson Oscillations in Layered Superconductors, *Phys. Rev. Lett.* **99**, 057002 (2007).
- [43] A. E. Koshelev, Alternating dynamic state self-generated by internal resonance in stacks of intrinsic Josephson junctions, *Phys. Rev. B* **78**, 174509 (2008).

- [44] S. Lin and X. Hu, Possible Dynamic States in Inductively Coupled Intrinsic Josephson Junctions of Layered High- T_c Superconductors, *Phys. Rev. Lett.* **100**, 247006 (2008).
- [45] V. M. Krasnov, Nonlinear Nonequilibrium Quasiparticle Relaxation in Josephson Junctions, *Phys. Rev. Lett.* **103**, 227002 (2009).
- [46] R. A. Klemm and K. Kadowaki, Output from a Josephson stimulated terahertz amplified radiation emitter, *J. Phys. Condens. Matter* **22**, 375701 (2010).
- [47] N. F. Pedersen and S. Madsen, THz generation using fluxon dynamics in high temperature superconductors, *IEEE Trans. Appl. Supercond.* **19**, 726 (2009).
- [48] X. Hu and S. Z. Lin, Cavity phenomena in mesas of cuprate high- T_c superconductors under voltage bias, *Phys. Rev. B* **80**, 064516 (2009).
- [49] T. Koyama, H. Matsumoto, M. Machida, and K. Kadowaki, In-phase electrodynamics and terahertz wave emission in extended intrinsic Josephson junctions, *Phys. Rev. B* **79**, 104522 (2009).
- [50] V. M. Krasnov, Coherent flux-flow emission from stacked Josephson junctions: Nonlocal radiative boundary conditions and the role of geometrical resonances, *Phys. Rev. B* **82**, 134524 (2010).
- [51] A. E. Koshelev, Stability of dynamic coherent states in intrinsic Josephson-junction stacks near internal cavity resonance, *Phys. Rev. B* **82**, 174512 (2010).
- [52] A. A. Yurgens, Temperature distribution in a large $\text{Bi}_2\text{Sr}_2\text{CaCu}_2\text{O}_{8+\delta}$ mesa, *Phys. Rev. B* **83**, 184501 (2011).
- [53] V. M. Krasnov, Terahertz electromagnetic radiation from intrinsic Josephson junctions at zero magnetic field via breather-type self-oscillations, *Phys. Rev. B* **83**, 174517 (2011).
- [54] M. Tachiki, K. Ivanovic, K. Kadowaki, and T. Koyama, Emission of terahertz electromagnetic waves from intrinsic Josephson junction arrays embedded in resonance LCR circuits, *Phys. Rev. B* **83**, 014508 (2011).
- [55] H. Asai, M. Tachiki, and K. Kadowaki, Three-dimensional numerical analysis of terahertz radiation emitted from intrinsic Josephson junctions with hot spots, *Phys. Rev. B* **85**, 064521 (2012).
- [56] S. Z. Lin and X. Hu, In-plane dissipation as a possible synchronization mechanism for terahertz radiation from intrinsic Josephson junctions of layered superconductors, *Phys. Rev. B* **86**, 054506 (2012).
- [57] Yu. O. Averkov, V. M. Yakovenko, V. A. Yampol'skii, and F. Nori, Conversion of Terahertz Wave Polarization at the Boundary of a Layered Superconductor due to the Resonance Excitation of Oblique Surface Waves, *Phys. Rev. Lett.* **109**, 027005 (2012).
- [58] B. Gross, S. Guénon, J. Yuan, M. Y. Li, J. Li, A. Ishii, R. G. Mints, T. Hatano, P. H. Wu, D. Koelle, H. B. Wang, and R. Kleiner, Hot-spot formation in stacks of intrinsic Josephson junctions in $\text{Bi}_2\text{Sr}_2\text{CaCu}_2\text{O}_8$, *Phys. Rev. B* **86**, 094524 (2012).
- [59] B. Gross, J. Yuan, D. Y. An, M. Y. Li, N. Kinev, X. J. Zhou, M. Ji, Y. Huang, T. Hatano, R. G. Mints, V. P. Koshelets, P. H. Wu, H. B. Wang, D. Koelle, and R. Kleiner, Modeling the linewidth dependence of coherent terahertz emission from intrinsic Josephson junction stacks in the hot-spot regime, *Phys. Rev. B* **88**, 014524 (2013).
- [60] H. Asai and S. Kawabata, Intense terahertz emission from intrinsic Josephson junctions by external heat control, *Appl. Phys. Lett.* **104**, 112601 (2014).
- [61] A. Grib and P. Seidel, The influence of external separate heating on the synchronization of Josephson junctions, *Phys. Status Solidi B* **251**, 1040 (2014).
- [62] F. Rudau *et al.*, Thermal and electromagnetic properties of $\text{Bi}_2\text{Sr}_2\text{CaCu}_2\text{O}_8$ intrinsic Josephson junction stacks studied via one-dimensional coupled sine-Gordon equations, *Phys. Rev. B* **91**, 104513 (2015).
- [63] F. Rudau, R. Wieland, J. Langer, X. J. Zhou, M. Ji, N. Kinev, L. Y. Hao, Y. Huang, J. Li, P. H. Wu, T. Hatano, V. P. Koshelets, H. B. Wang, D. Koelle, and R. Kleiner, Three-Dimensional Simulations of the Electrothermal and Terahertz Emission Properties of $\text{Bi}_2\text{Sr}_2\text{CaCu}_2\text{O}_8$ Intrinsic Josephson Junction Stacks, *Phys. Rev. Applied* **5**, 044017 (2016).
- [64] D. P. Cerkoney, C. Reid, C. M. Doty, A. Gramajo, T. D. Campbell, M. A. Morales, K. Delfanazari, M. Tsujimoto, T. Kashiwagi, T. Yamamoto, C. Watanabe, H. Minami, K. Kadowaki, and R. A. Klemm, Cavity mode enhancement of terahertz emission from equilateral triangular microstrip antennas of the high- T_c superconductor $\text{Bi}_2\text{Sr}_2\text{CaCu}_2\text{O}_{8+\delta}$, *J. Phys. Condens. Matter* **29**, 015601 (2017).
- [65] R. A. Klemm, A. E. Davis, and Q. X. Wang, Terahertz emission from thermally managed square intrinsic Josephson junction microstrip antennas, *IEEE J. Sel. Top. Quantum Electron.* **23**, 1 (2017).
- [66] V. P. Koshelets, P. N. Dmitriev, M. I. Faley, L. V. Filippenko, K. V. Kalashnikov, N. V. Kinev, O. S. Kiselev, A. A. Artanov, K. I. Rudakov, A. De Lange, G. De Lange, V. L. Vaks, M. Y. Li, and H. B. Wang, Superconducting integrated terahertz spectrometers, *IEEE Trans. Terahertz Sci. Technol.* **5**, 687 (2015).
- [67] H. Eisele, M. Naftaly, and J. R. Fletcher, A simple interferometer for the characterization of sources at terahertz frequencies, *Meas. Sci. Technol.* **18**, 2623 (2007).
- [68] E. Sobakinskaya, V. L. Vaks, N. Kinev, M. Ji, M. Y. Lia, H. B. Wang, and V. P. Koshelets, High-resolution terahertz spectroscopy with a noise radiation source based on high- T_c superconductors, *J. Phys. D* **50**, 035305 (2017).
- [69] T. Uno and H. Tabata, *In situ* measurement of combustion gas using terahertz time domain spectroscopy setup for gas phase spectroscopy and measurement of solid sample, *Jpn. J. Appl. Phys.* **49**, 04DL17 (2010).
- [70] V. P. Koshelets and S. V. Shitov, Integrated superconducting receivers, *Supercond. Sci. Technol.* **13**, R53 (2000).
- [71] G. de Lange *et al.*, Development and characterization of the superconducting integrated receiver channel of the TELIS atmospheric sounder, *Supercond. Sci. Technol.* **23**, 045016 (2010).
- [72] N. V. Kinev, L. V. Filippenko, K. V. Kalashnikov, O. S. Kiselev, V. L. Vaks, E. G. Domracheva, and V. P. Koshelets, Superconducting integrated terahertz receiver for spectral analysis of gas compounds, *J. Phys. Conf. Ser.* **741**, 012169 (2016).
- [73] Note that the amplitudes of the signals detected in experiments 1 and 2 (Figs. 3 and 4) are difficult to compare

since the measurements are done with very different receiver input bandwidths. The wideband receiver of experiment 1 integrates the power emitted by the BSCCO emitter at different frequencies; thus, the absorption is much lower than the calculations and measurements associated with the SIR, having a spectral resolution well below the gas lines at all gas pressures displayed.

- [74] E. Gerecht, K. O. Douglass, and D. F. Plusquellic, Chirped-pulse terahertz spectroscopy for broadband trace gas sensing, *Opt. Express* **19**, 8973 (2011).
- [75] L. Consolino, S. Bartalini, H. E. Beere, D. A. Ritchie, M. Serena Vitiello, and P. De Natale, THz QCL-based cryogenic-free spectrometer for *in situ* trace gas sensing, *Sensors* **13**, 3331 (2013).